PCCP

Accepted Manuscript

ROYAL SOCIETY OF CHEMISTRY

www.rsc.org/pccp

Graphene/CdS Quantum Dots/Polyoxometalate Composite Films For Efficient Photoelectrochemical Water splitting and Pollutant Degradation

Meng Wang, [a,b]Xinke Shang[a,b], Xuelian Yu[a], Rongji Liu[a], Yongbin Xie[a], He Zhao[a], Hongbin Cao[a] and Guangjin Zhang [a]*

[a] *Key laboratory of Green Process Engineering, Institute of Process Engineering, Chinese Academy of Science, 100190, Beijing, China*

[b] *University of Chinese Academy of Sciences, 100049, Beijing, China*

*corresponding author. Email address: zhanggj@ipe.ac.cn

Abstract: The rGO/CdS/H2W12 nanocomposite film was successfully fabricated by the layer-by-layer self-assembly method. The composite film was characterized by UV-Vis spectra, XPS, AFM etc. The composite film showed high photoelectronic response under illumination of sun light. Both current−voltage curves and photocurrent transient meaurement demonstrated that the photocurrent response of the rGO/CdS/H2W12 composite film was enhanced by 5 times compared with CdS film. This can be attributed to the photoinduced electron transfer between CdS, H2W12 and rGO, which promotes the charge separation efficiency of CdS. The introduction of GO enhanced the charge separation and transportation. More importantly, various pollutant can be treated as electron donor and thus been degraded and production of hydrogen in the same time at low bias voltage under irradiation of solar light.

Key words: photoelectrocatalysis, water splitting, CdS quantum dot, polyoxometaltes, pollutant degredation

1. Introduction

In the past decade, the serious world's energy and environmental crisis make people pay more attention on the development of sustainable carbon-neutral energy. As an efficient energy carrier with the highest energy density values per mass of 140MJ/kg, hydrogen represents a green fuel of the further. The current main production of hydrogen comes from the petroleum industry, which consume the nature resources and generate CO_2. Thus to generate hydrogen by photocatalysis(PC) or photoelectrocatalysis (PEC) from water splitting under solar light irradiation is anticipated as promising further technology to solve the energy crisis[1]. In another hand, the photocatalysis or photoelectrocatalysis can also be used to degradation of inorganic/organic pollutant, which also provide a new route to solve the environmental crisis[2]. The process is as follows: a semiconductor catalyst is excited by the photons and generates electron-hole pairs. The holes can oxidize the target organic/inorganic substance and liberating hydrogen ions. The hydrogen ions are in turn reduced by the excited electrons to form molecular hydrogen. In such a process, pollutant can be regarded as resources for hydrogen evolution in water splitting. Various pollutants can be used as the target substance, such as S^{2-}, alcohols, phenols, PVA etc, which are rich in the waste water from many plant including metallurgy industry, wine industry, coal chemical industry, textile and paper industry and so on.

Compared with PC, the PEC is more efficient and effective since it use photoanode as the working electrode instead of directly introducing the catalyst in the waste water. For PEC, the primary requirement for high solar energy conversion is that the photoanode material should have good photoelectrochemical response ability in the spectrum of solar light, besides its high stability

in the electrolyte. Considerable efforts have been exerted on the synthesis and photoelectrochemical test of semiconductor quantum dots thin films, due to their good visible light absorption performance and low production cost[3]. Among all the materials, CdS quantum dots (QDs) is a fascinating compound due to its excellent properties in that the band gap (2.4 eV) corresponds well with the spectrum of sunlight and the conduction band edge is more negative than the H_2O/H_2 redox potential.[4–6] However, for the single CdS, the biggest stumbling block is its dissatisfactory quantum efficiency, which is greatly limited by a high electron−hole recombination rate and a low photogenerated charge transfer rate. In order to solve these problems, many strategies such as morphological control, semiconductor coupling, and combination with other materials have been adopted.[7–10] Among them, the most promising approach is constructing composite thin films, in which the photogenerated electron from the CdS quantum dots could quickly transfer to other materials that served as electron acceptor to synergically and effectively retard the fast charge pair recombination and consequently enhance the overall photoefficiency. Recently, Liu et al have prepared CdS QD/graphene composite film by layer-by layer method and they found that incoration of graphene enhanced the photocurrent of CdS QDs. [11]

Polyoxometalates (POMs), the early transition metal oxygen anionic clusters have shown uniquely physicochemical properties that can accept multielectrons while retaining intact structure.[12] The CB level of CdS (−0.8 V versus NHE) is more negative than the 2e reduction potential of most POMs, which enables the transfer of stimulated electron from CB of CdS to POMs. Recently, POMs have been successfully introduced into photoanode composite thin films coupling with CdS quantum dots to promote the photocurrent response.[13] However, in such POM/CdS QD system, electrons accepted by POMs have no outlet and the poor conductivity of

the hybrid film inhibits the enhancement of photoelectrochemical response. In recent years, graphene has been regarded as an important building block for synthesizing various functional photoanodes, owing to its extraordinary properties with a high charge-carrier mobility and stability.[14-18] The graphene-polyoxometalate nanomaterials also showed enhanced photoelectrochemical response and it is worth noting that rGO or graphene in the composite thin films can be produced by in situ photoreduction of GO in the presense of polyoxometalates.[19] Thus, it is highly desirable that incorporating POMs and graphene into CdS quantum dots film may be an effective way to facilitate photogenerated electron transfer and promote the photocurrent response. To our knowledge, such rGO/CdS/POM composite films have never been constructed and their photoelectrochemical performance has been virtually unexplored so far.

Herein, we report for the first time the self-assembled multilayer (SAM) thin films of GO, CdS quantum dots and ammonium metatungstate ($(NH_4)_6H_2W_{12}O_{40}$, denoted as H2W12) which were fabricated by the layer-by-layer (LbL) self-assembly method. An in situ photoreduction protocol was adopted to convert GO to rGO due to the photocatalytic activity of H2W12 (Scheme 1). Photoelectrochemical test showed that the rGO/CdS/H2W12 composite films showed the best PEC performance with photocurrent reaching 0.8mA/cm^2 under illumination of simulated solar light, which is almost 5 times of that of CdS SAM film. To the best of our knowledge, this is the first report that exhibit the idea of co-introduction of both POM and rGO to CdS QDs, which can facilitate the charge separation in CdS QDs and thus enhance its photocatalytic activities.

2. Experimental Section

2.1 Materials

Poly-(styrenesulfonate) (PSS, MW 70000), 3-aminopropyltrimethoxysilane (APS), Poly(allylamine hydrochloride) (PAH, MW 15000), ammonium metatungstate (H2W12) were purchased from Aldrich Chemical Company. All other reagents were of analytical grade. Ultrapure water purified with Milli-Q (MQ) plus system (Millipore Co.) with resistivity of 18.2 MΩcm was exclusively used in all aqueous solutions and rinsing procedures.

2.2 Synthesis of CdS quantum dots

Amine-modified CdS QDs were synthesized as follows: chlorinated cadmium (CdCl2, 0.9166 g, 5 mmol), 2-mercaptoethylamine hydrochloride (1.42 g, 12.5 mmol), and sodium sulfide nonahydrate (1.5011 g, 6.25 mmol) were dissolved in deionized water (250 ml). The reaction proceeded at 40℃ for 5 h and then at 60℃ for 5 h under vigorous stirring. The resulting solution was a homogeneous yellow colloid suspension. After the solution was cool, then isopropyl alcohol was added and the solution became turbid, and the yellow precipitate was separated by centrifugation. After isolation, the precipitate was dissolved again in water and re-precipitated with isopropyl alcohol. This operation was repeated a further two times. Finally, the precipitate of amine-modified CdS QDs was dried in vacuum at 40℃ for 1 day.

2.3 Layer-by-layer assembly of GO/CdS quantum dots/polyoxometalate composite films

GO (graphene oxide) was oxidized from NG flakes by a modified Hummers method using H_2SO_4, $NaNO_3$ and $KMnO_4$ in an ice bath as reported in great detail elsewhere. The resulting homogeneous brown GO dispersion was tested to be stable for several months and used for reduction. The pH value of GO solution is ~ 7 and its zeta potential is about -40 mV, which means that GO are negatively charged.S4 Quartz substrates, silicon wafers, and indium tin oxide (ITO)-coated glass were cleaned as follows: the substrate was sonicated in a mixture of

ethanol/H2O (1:3) and acetone/H2O (1:3) for 20 min, respectively, and finally rinsed with distilled water prior to use. The fabrication procedure of GO/CdS quantum dots/polyoxometalate multilayer films is shown schematically in Scheme 1. A cleaned substrate was immersed into the APS solution for 8 h, then immersed in HCl (pH = 2.0) for 20 min to form the positive charged precursor film, followed by washing with deionized water and drying in nitrogen. Then, the substrate-supported precursor film was alternately dipped into the GO (0.3mg mL-1) water solution, CdS (2mg mL^{-1}) quantum dots solution, H2W12 (1mg mL^{-1}) solution, and PAH (2mg mL^{-1}) solution for 15 min, and rinsed with deionized water and dried in nitrogen after each dipping. Finally, $(GO/CdS/H2W12)_n$ self-assembled multi-layer (SAM) films were obtained by repeating these procedures (n is the deposited number of layers). For comparison, $(PSS/CdS/H2W12)_6$ and $(PSS/CdS/PSS)_6$ SAM films were prepared in a similar way and denoted as CdS/H2W12 SAM film and CdS SAM film for clarity.

2.4 Generation of $(rGO/CdS/H2W12)_6$ films by photoreduction

The substrates coated by GO/CdS/H2W12 films were placed 10 cm in front of a 100 W high-pressure mercury lamp equipped with a water filter and a WG280 cut-off filter. The photoreduction was carried out with 5 min in air atmosphere. An airflow cooling system was used to keep the samples at room temperature.

2.5 Characterization

Transmission electron microscopy (TEM) images were obtained using a JEM-2010 transmission electron microscope at an acceleration voltage of 200 kV. X-ray photoelectron spectroscopy (XPS) measurements were performed in ultrahigh vacuum (UHV) with Krato, AXIS-HS monochromatized Al Kα cathode source, at 75–150 W, using low energy electron gun for charge

neutralization. Atomic force microscopy (AFM) images were recorded on Leica TCS SP 5. Scanning electron microscope (SEM) was conducted on JSM 6700F. UV-vis absorption spectra were recorded on a Perkin-Elmer Lambda 350 spectrophotometer. For the photoluminescence (PL) spectrum, the samples were excited by 360 nm pulses generated from a Raman shifter on a Hitachi F-7000 fluorescence spectrophotometer. Cyclic Voltammetry (CV) measurements were performed on a CHI660D Electrochemical Workstation (Shanghai Chenhua Instrument Corp., China) at room temperature. A standard three-electrode cell was used and was controlled at room temperature. A platinum foil (3.0 cm^2) and saturated calomel electrode (SCE) were used as counter and reference electrode, respectively. The prepared multilayer film was used as the working electrode. 0.1 M phosphate buffer solution at pH 8.0 was used as the electrolyte.

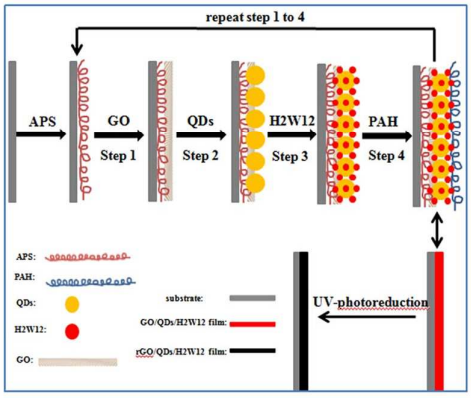

Scheme1: Scheme 1 Schematic illustration of the fabrication procedure of GO/CdS QDs/H2W12 multilayer films and a subsequent in situ photoreduction to convert GO to rGO.

2.6 Photoelectrochemical experiment

All photoelectrochemical experiments were performed on a CHI660D Electrochemical Workstation (Shanghai Chenhua Instrument Corp., China) at room temperature. The photocurrent intensity versus measured potential (I-V curve) measurements and photocurrent transient experiments were performed in a standard three-electrode configuration. The (rGO/CdS/H2W12)6

films on ITO electrode was used as the working electrode, a platinum foil (3.0 cm^2) and saturated calomel electrode (SCE) were used as counter and reference electrode, respectively. A simulated solar light lamp with the available spectral range from 350-760 nm (AM 1.5G) was used as the light source. Films were deposited on both sides of the ITO surface, but the conductive side was oriented facing the light. The illumination area of the working electrode was set constant at 1 × 1 cm^2. Photocurrent transient experiments were carried out at a constant bias of -0.4 V. All photoelectrochemical measurements were done in a 1 M Na_2S electrolyte to maintain the stability of the CdS particles.

2.7 Degradation of pollutant

All the degradation experiments were performed in the same cell of the PEC experiments. Various model pollutants with certain concentration (listed in Table 1) were put in the electrolyte. During the degradation of MO, the working electrode was held at 0V Vs SCE under irradiation of same light source of PEC experiment. The concentration of MO during the degradation process was determined by UV-visible spectra. The degradation process was fit by using first order reaction kinetics equation: $\ln (C_0/C)=kt$, where C_0 is the initial concentration of MO, C is the concentration of MO during the degradation process, k is the rate constant and t is the degradation time.

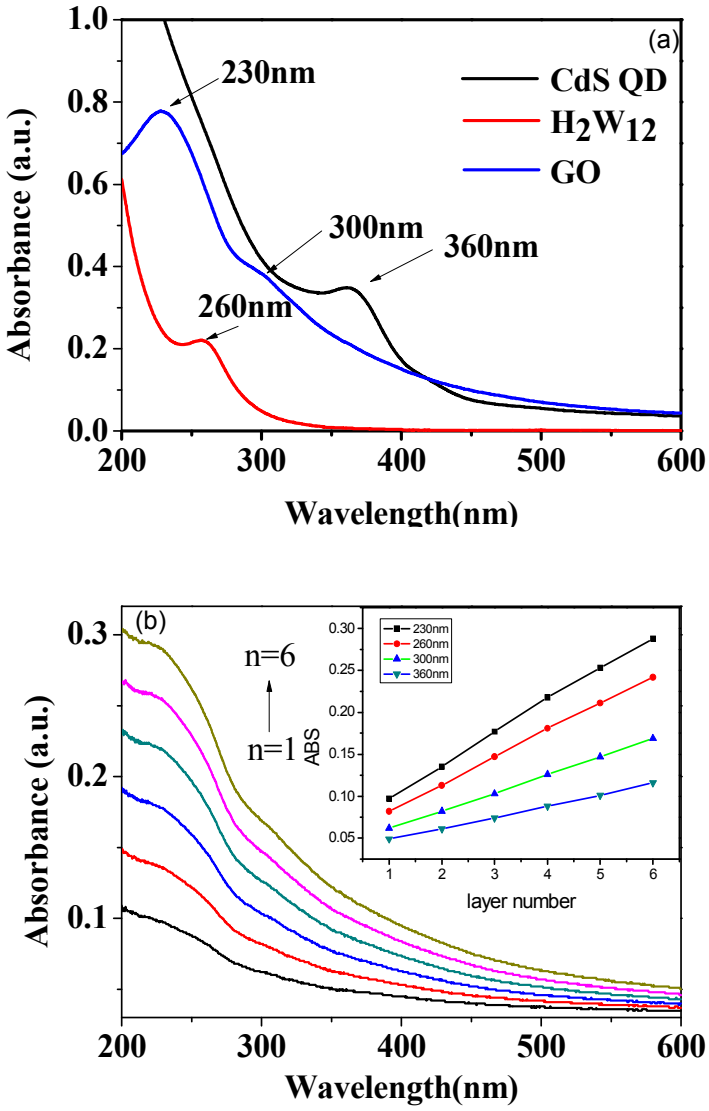

Figure 1 (a) UV-Vis absorption spectra of aqueous 0.01 mg/mL CdS solution (black line), aqueous 0.05 mg/mL GO solution (blue line) and aqueous 0.05 mg/mL H2W12 solution (red line). (b) UV-Vis absorption spectra of (GO/CdS/H2W12)n SAM films with layer number n=1-6 on a quartz substrate, which was modified before by a APS precursor film. The curves, from bottom to top, correspond to n=1-6. Inset: plots of the absorbance values at 230, 260, 300 and 360 nm as a function of the layer number n.

3. Results and discussions

3.1 characterizations of multi-layer hybrid film

Scheme 1 shows the assembly process in water solution, the electrostatic interaction is the driving force, owing to the negatively charged surface of GO[20] and H2W12 clusters, the positively charged surface of CdS quantum dots[21] and poly(allylamine) hydrochloride (PAH). First, the substrates were modified by a protonated 3-aminopropyltrimethoxysilane (APS) layer as precursor film, and then different numbers of GO/CdS/H2W12 layers were deposited on the modified substrates to construct multilayer films, in which each layer was linked by PAH layers. In such a film structure, the H2W12 clusters adsorb heavily with the GO layers. This design aims to realize an effective interaction between oxygen-containing groups on GO and H2W12 clusters, which is favorable for the electron transfer from photoexcited H2W12 to GO, thus realizing an efficient reduction of GO in the subsequent H2W12-assisted photoreduction process. GO, CdS and H2W12 all show characteristic absorptions in the UV-Vis region, as presented in Figure 1a. Two absorption bands of GO appear at 230 and 300 nm respectively. CdS has the absorption peak at 360 nm while that of the H2W12 is located at 260 nm. Therefore, it is easy to monitor the formation of GO/CdS/H2W12 multilayer films by UV-Vis spectroscopy, according to the film absorbance at the characteristic absorption bands of GO, CdS and H2W12. Figure 1b displays the UV-Vis absorption spectra of $(GO/CdS/H2W12)_n$ multilayer films (with n=1-6) assembled on quartz substrates. The absorption of the films increases systematically with the layer number n, which is an evidence for the subsequent deposition of GO, CdS and H2W12 components. The absorption in the visible region is attributed to the adsorbed CdS. The excitonic peak of CdS at 360 nm indicates the formation of ca. 2.5 nm particles.[21] Transmission electron microscopy (TEM)

image (shown in Figure S1, ESI†) revealed that most CdS particles are in the size of 2.4-3.0 nm, which is consistent with the estimate from absorption spectra. The absorbance values for (GO/CdS/H2W12)n multilayer films with n=1-6 at 230, 260, 300 and 360 nm are plotted as the function of the layer number n, as shown in the inset of Figure 1b. Apparently, the absorbance varies linearly with n at all four wavelengths, which reveals a constant increase in the total amount of GO, CdS and H2W12 adsorbed in the films after each deposition cycle of GO/CdS/H2W12 layer. Furthermore, the Cyclic Voltammetry (CV) measurement characteristics of (GO/CdS/H2W12)n multilayer films (with n=1-6) featured in Figure 2 also confirm the growth of absorbed H2W12 after each deposition cycle. There are two pairs of reversible redox peaks between the potential range from -1.0 V to 0 V Vs SCE (shown in Figure S2, ESI†) for H2W12 under 0.1 M phosphate buffer solution, which refers to 1e reduction potential (-0.65 V) and 2e reduction potential (-0.79 V) respectively.[22] For $(GO/CdS/H2W12)_n$ multilayer films (with n=1-6) absorbed on ITO, the current increases systematically and the reversible redox peaks appear clearly with the layer number n. The current values for (GO/CdS/H2W12)n multilayer films with n=1-6 at peak potential -0.59, -0.79, -0.65 and -0.86 V are plotted as the function of the layer number n, as shown in the inset of Figure 2. Apparently, the current varies linearly with n at all four peak potentials, which is an evidence for the subsequent deposition of H2W12 component.

An in situ photoreduction of the film was employed to convert the GO into conductive rGO. The detailed procedure of photoreduction of GO/CdS/H2W12 films is shown in the experimental section. In the photoreduction procedure, the GO/CdS/H2W12 multilayer films were irradiated by a 100 W high-pressure mercury lamp to oxidize the organic polyelectrolytes and reduce the GO by using the photocatalytic activity of H2W12 clusters.[23] Under the irradiation of UV light, the O-W

charge-transfer band in the H2W12 cluster is excited, which leads to electron-hole separation.[24] The excited H2W12 clusters act as both oxidant and reductant. PAH is oxidized by excited H2W12 and the electrons trapped by excited H2W12 clusters are transfered to GO, resulting in the reduction of GO. After photoreduction, the color of the films gradually turned from light brown to black (shown in Figure S3, ESI†), suggesting the successful formation of rGO. In the whole photoreduction process, H2W12 acts as a photocatalyst and an electron relay.[24,25] This process can be described as

H2W12 + hv → H2W12（h + e）

H2W12（h + e）+ PAH → H2W12（e）+ oxidized PAH

H2W12（e）+ GO → H2W12 + rGO

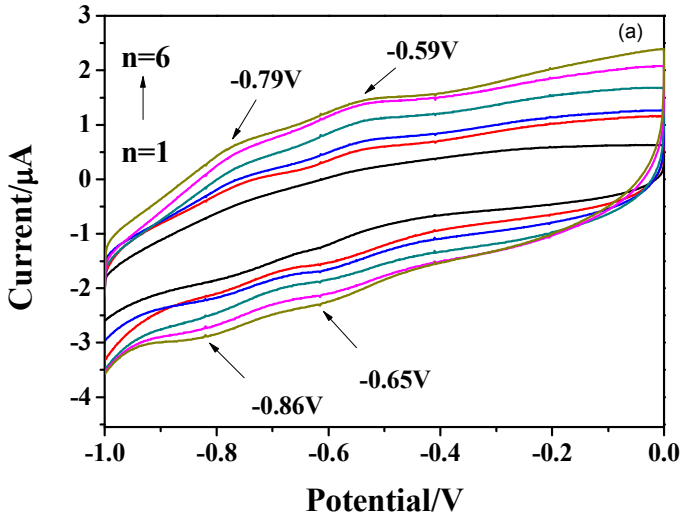

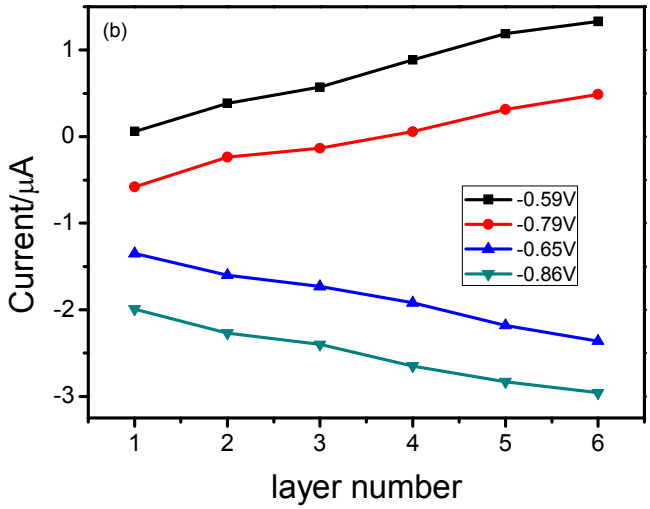

Figure 2 (a)Cyclic Voltammetry curves of (rGO/CdS/H2W12)n multilayer films (with n=1-6) in the electrolyte of 0.1 M phosphate buffer solution. (b) plots of the current values at peak potential -0.59, -0.79, -0.65 and -0.86 V as a function of the layer number n.

X-ray photoelectron spectroscopy (XPS) was employed to further prove the successfully fabrication of GO, CdS and H2W12 components and analyze the compositional change of carbon atoms and CdS in different chemical states of GO/CdS/H2W12 films before and after photoreduction. Figure 3(a-b) shows the C 1s XPS spectra before and after UV irradiation. Four types of carbon with different chemical states are observed, which appear at 284.8 eV for graphite-like C, 286.8 eV for C–O, 287.8 eV for C=O and 288.8 eV for O–C=O. After the photoreduction, the content of C–O group decreases from initial 31.2% to 18%, indicating that the photoreduction can effectively eliminate the oxygen containing groups on GO. Meanwhile, the content of C-C/C=C group increased from 67.8% to 81.2%, indicating that significant sp3/sp2-hybridized carbon structures were restored. The Cd 3d and S 2p XPS spectra are shown in Figure 4(a-d). The contents of Cd and S didn't change significantly after UV irradiation, for the atomic percent varies from 0.08% to 0.07% for Cd and S elements, indicating that the CdS is

stable and present after photoreduction. The presence of W was proved by XPS as shown in Figure S4, ESI†. These results further confirm that we indeed incorporate GO, CdS and H2W12 into the composite films and finally obtain rGO/CdS/H2W12 SAM films without destruction.

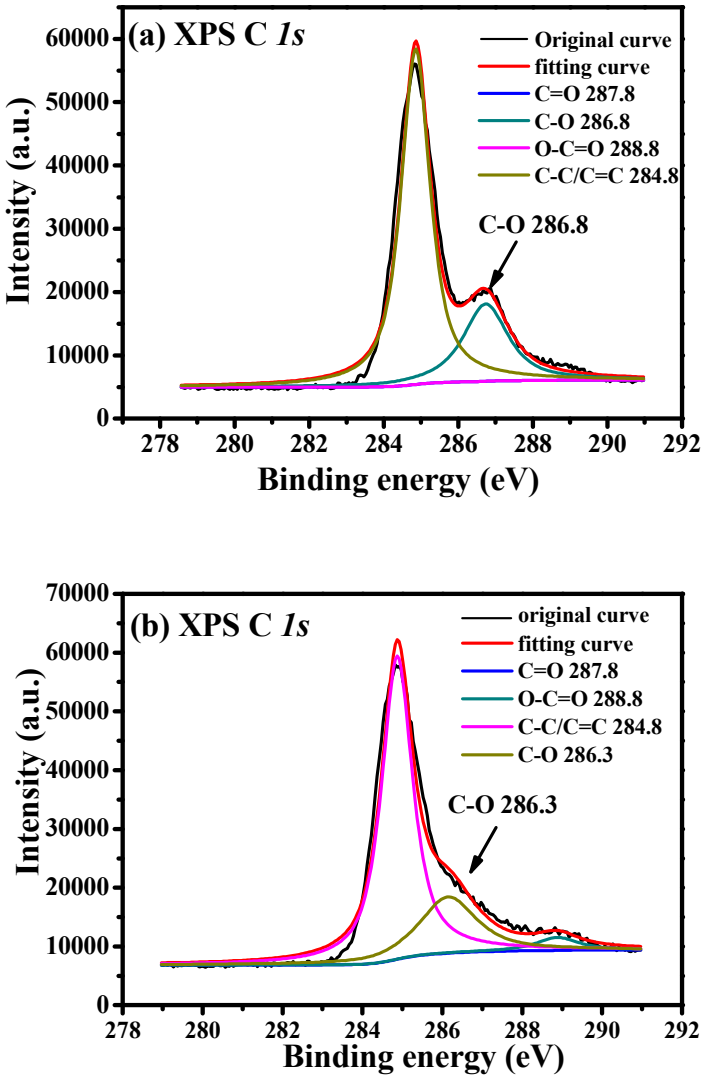

Figure 3 C 1s XPS spectra of a (GO/CdS/H2W12)6 film on quartz substrate before (curve a) and after (curve b) 5 min of UV photoreduction.

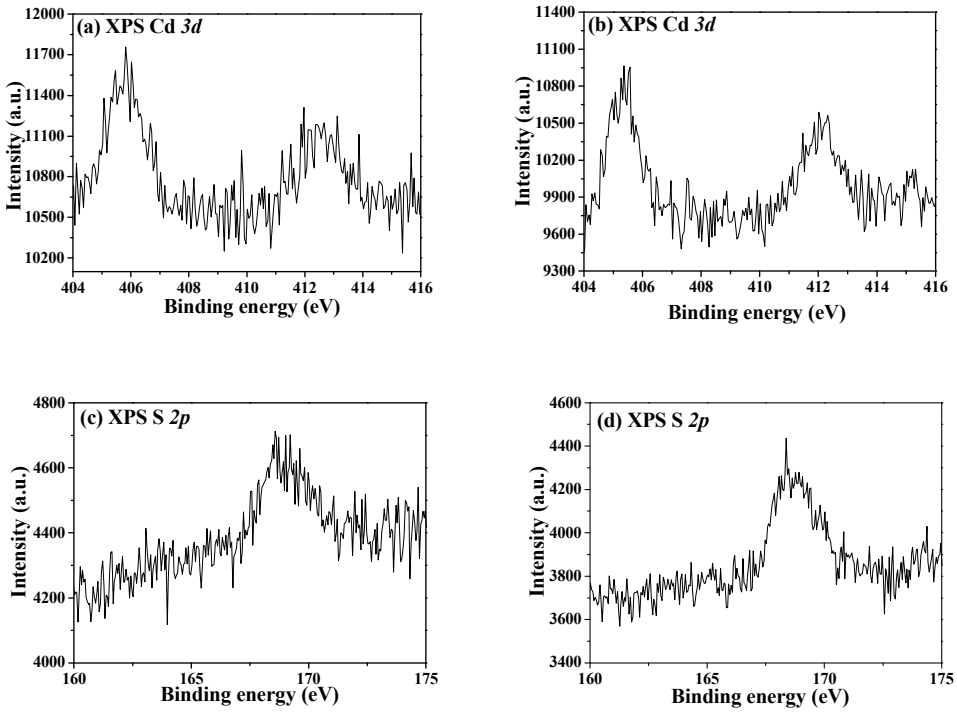

Figure 4 XPS spectra of Cd 3d and S 2p of rGo/CdS/H2W12 SAM film before (a, c) and after (b, d) UV irradiation

The surface morphology of the rGO/CdS/H2W12 film was characterized by atomic force microscopy (AFM) and scanning electron microscope (SEM) measurement. The AFM image (shown in Figure S5, ESI†) shows typical spherical or pillar patterns, which is due to the aggregation behavior of CdS or H2W12 particles. The aggregated particles are uniformly distributed and the mean diameter is ca. 70 nm. In addition, the thickness of the film is ca. 30 nm observed from three-dimensional AFM images. The SEM image (shown in Figure S6, ESI†) also shows that the film surface consists of a multitude of small domains and the distribution is uniform. The domains are ascribed to the H2W12 clusters adsorbed on PAH chains and the relatively uniform morphology is an intrinsic advantage of the LBL assembly method, which further determines the excellent photoelectric performance. The cross section image of the film

showed the layered structure and the thickness of the film is about 1 μm (Figure S7).

3.2 PEC performance of the composite films

Figure 5a shows the current−voltage curves of the SAM films photoelectrode. For comparison, the layer number of all the films was kept as 6. For the CdS SAM film, the onset potential is -0.30 V versus SCE, while those of CdS/H2W12 SAM film and rGO/CdS/H2W12 SAM film photo-electrodes are -0.70 and -0.65 V, respectively. The onset potential of the rGO/CdS/H2W12 SAM film photoelectrode is obviously more negative than those of the other two, demonstrating a shift in Fermi level to more negative potential as a result of coupling between CdS, H2W12 and rGO in the composite system. To investigate the photoelectrochemical performance of the LbL films, photocurrent transient experiments have been carried out under simulated solar light irradiation at the bias voltage -0.2V vs SCE. As shown in Figure 5b, all the films represent fast anodic photocurrent responses when the irradiation is switched on and off. The photocurrent response intensity increases as follows: the CdS SAM film < the CdS/H2W12 SAM film < the rGO/CdS/H2W12 SAM film. The CdS SAM film displays the lowest photocurrent (ca. 0.17mA/cm^2 at 0V vs SCE), which is not surprising due to the fast charge pair recombination. The introduction of H2W12 induces a stronger photocurrent response (ca. 0.4 mA/cm^2 at 0V vs SCE). However, the rGO/CdS/H2W12 SAM film shows the strongest photocurrent response (ca. 0.8mA/cm^2 at 0V vs SCE) and the photocurrent response intensity is larger than the algebraic summation of the others, suggesting that a synergic effect occurs between CdS, H2W12 and rGO. The comparison of photocurrent with rGO/CdS, rGO/H2W12, rGO and H2W12 SAM films was also performed and shown in Figure S8. For rGo/CdS, it showed better performance than CdS

SAM film. But for rGO/H2W12, rGO and H2W12 SSAM film, they do not show any photocurrent under same experiment conditions.

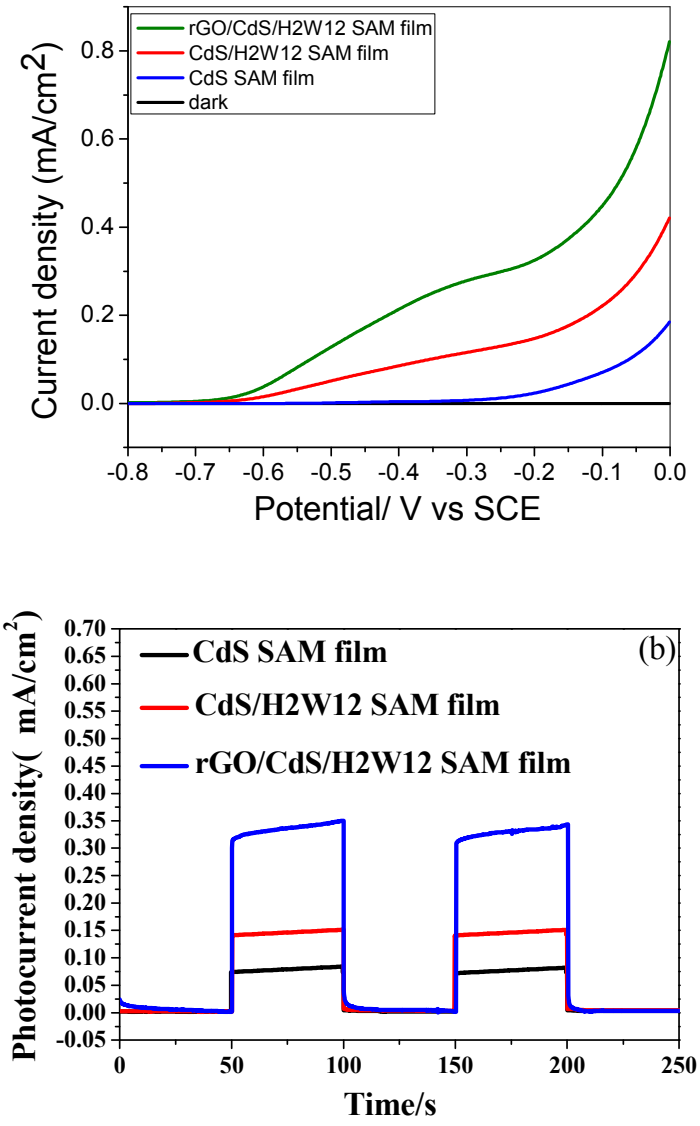

Figure 5 I-V curves (a) and photocurrent responses at bias of -0.2V vs SCE (b) of the different photoelectrodes. The photocurrents were measured versus SCE under simulated sunlight with an illumination intensity of 100 mW/cm^2 in 1 M Na_2S aqueous solution.

3.3 Degradation of pollutant

The favorable electron separation and transport properties of the composite films were further supported by pollutant degradation experiments. In the above experiments, S^{2-} that is rich in waste water of metallurgy industry was used as the hole consumption agent, which showed high output photocurrent. Other organic compound were also selected as the hole consumption agent, including alcohol, phenol, dyes, surfactant, ammonia etc. [26] The results are summarized in Table 1. It can be observed that both methanol and ethanol can give good photocurrent output with negative onset potential. Organic dyes such as MO can also generate good photocurrent although a little bit lower than S^{2-} and alcohols. Phenol can also give substantial currents as well as PVA and ammonia. Among all the compounds, surfactant induces much lower currents, indicating the difficulty of degradation of such compound. It can be concluded that the composite film can be used as an efficient photoanode to degradation of most organic pollutant and generate hydrogen at the same time.

Finally, MO was used as represent target pollutant to study its degradation process by monitoring the decrease of its typical absorption. For comparison, direct photolytic degradation of MO in aqueous solution was also performed. The results were shown in Figure 6. The PEC electrolysis was performed under bias of 0V vs SCE. It can be seen that all the three SAM films showed activities to degradation of MO, but with different reaction rate. As shown in Figure 6b, the rGO/CdS/H2W12 SAM film showed the best performance in degradation of MO with reaction rate constant of ~$0.88h^{-1}$. This rate constant of PEC degradation of MO is found to be 3 times higher than that for CdS/H2W12 SAM film with constant of $0.31h^{-1}$ and nearly 5 times higher than that for CdS SAM film with the constant of $0.18h^{-1}$. These results further supported the enhanced separation of photo-generated electron-hole pairs in the composite films.

The stability of the photoanode was also studied by reusing this electrode in three PEC cycles. No obvious degradation of performance was found and the results are reproducible in three PEC cycles.

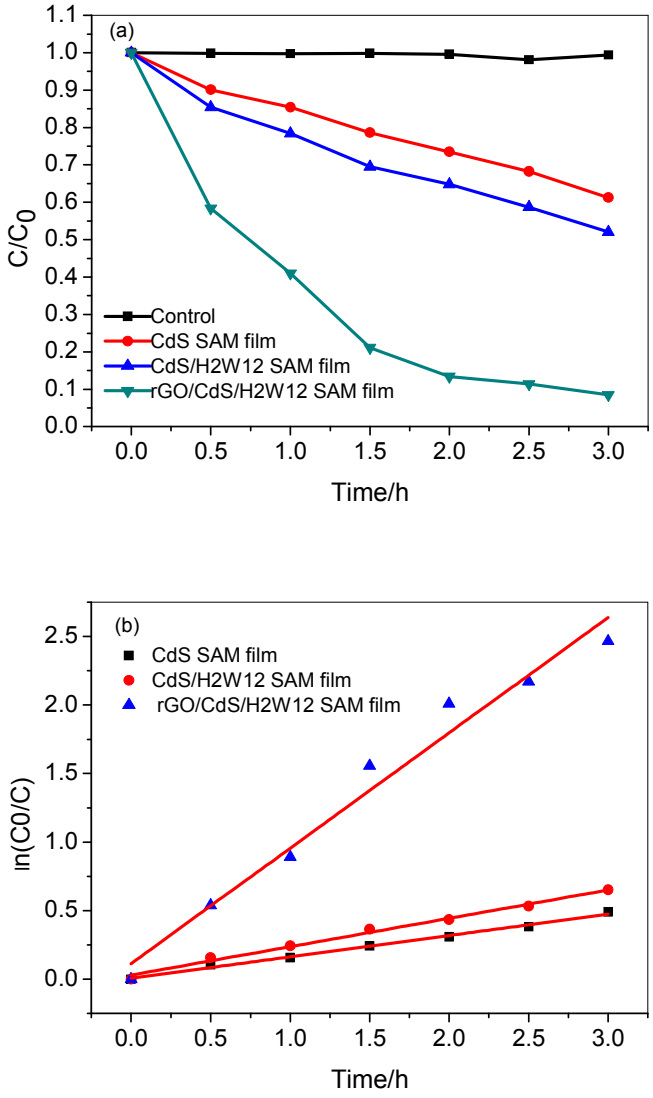

Figure 6 (a) PEC degradation of MO solutions by different films; (b) kinetic curves of degradation of MO by different films

3.4 Discussions

In consideration of the reduction potential of H2W12 (-0.337 V versus normal hydrogen electrode

(NHE)), the CB level of CdS (−0.8 V versus NHE), and the zero gap semiconductor of graphene,[13] the electron transfer from the CdS CB to H2W12 and then to rGO is a favorable exothermic process. When the SAM film is fabricated with CdS, H2W12 and rGO, CdS photogenerated electrons in the excited state can be extracted and transferred to the H2W12, then quickly delivered to the rGO. This process can effectively retard the fast electron−hole recombination on the surface of CdS, consequently improving the photoelectrochemical performance. To further discuss the mechanism of the photocurrent generation, the photoluminescence (PL) spectra of the prepared films were investigated. As shown in Figure 7, the CdS SAM film exhibits a broad PL band centered at 430 nm. While, the intensity of CdS/H2W12 SAM film remarkable decreased. With introduction of GO, the PL of rGO/CdS/H2W12 film was further eventually quenched, which illustrated that rGO can effectively facilitate charge propagation from the conduction band of semiconductors to the electrode. The facilitated charge separation can further be confirmed by the lifetime measurement. As shown in Figure S5, the average lifetime of SAM film decreased from 12ns for CdS SAM film decreased to about 7ns for CdS/H2W12 SAM film and then further deceased to 4 ns for rGO/CdS/H2W12 SAM film.

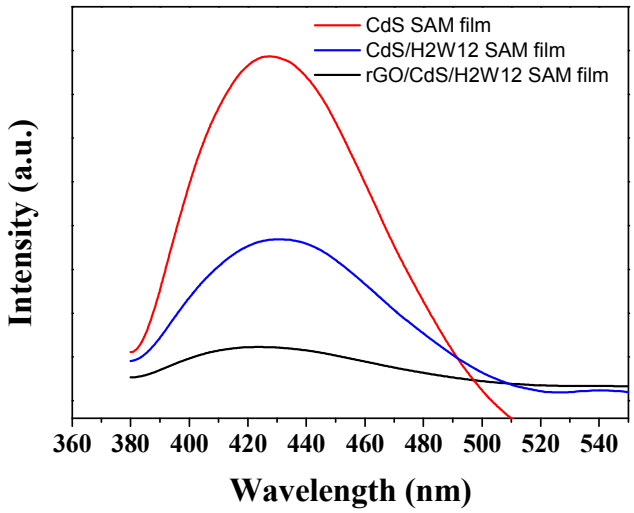

Figure 7 Photoluminescence spectra of the different SAM film obtained upon excitation at 360 nm.

Therefore, the enhancement of the photocurrent can be attributed to strong photoinduced electron transfer interactions between CdS, H2W12 and rGO in the films. From the above results, the mechanism for the photocurrent generation is proposed in Scheme 2 as follows: Under the simulated solar light illumination, CdS absorbs visible light and generates electron−hole pairs. The photogenerated electrons transfer from the CB of CdS into H2W12, and then the electrons transfer from H2W12 to rGO and ultimately to ITO linked with the external circuit. The holes left in CdS were consumed by S^{2-} exist in the electrolyte.

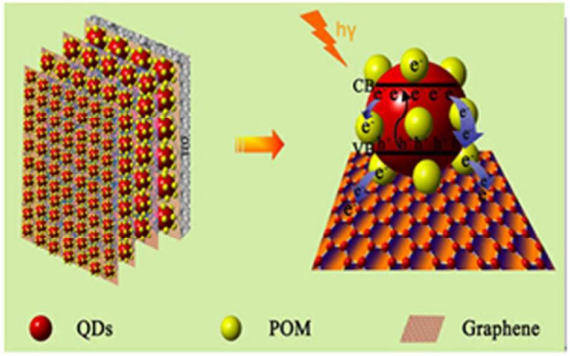

Scheme 2 The proposed mechanism of the photocurrent generation of rGO/CdS/H2W12

composite system.

Table 1 PEC characteristics under solar light illumination for various pollutants

Target pollutant	Onset potential (V vs SCE)	Current density at 0V vs SCE (mA/cm^2)
S^{2-}	-0.70	0.80
Methanol (10% v.)	-0.66	0.75
Ethanol (10% v.)	-0.64	0.72
MO(20mg/L)	-0.61	0.60
Phenol (10% v.)	-0.58	0.46
PVA (20mg/L)	-0.60	0.49
Ammonia (1% v.)	-0.54	0.46
SDS(0.05mol/L)	-0.30	0.21

4. Conclusions

In conclusion, the rGO/CdS/H2W12 SAM film was successfully fabricated by the LbL self-assembly method. Both current−voltage curves and photocurrent transient measurement demonstrated that the photocurrent response of the rGO/CdS/H2W12 SAM film increased by 5 times in comparison with the CdS SAM films. The photoinduced electron transfer between CdS, H2W12 and rGO, which promotes the charge separation efficiency of CdS, lead to such enhancement of photocatalytic activities. The introduction of rGO in the composite film facilitates the charge separation and transportation during PEC process. This work would pave a new way for design of efficient photoanode system for water splitting and pollutant degradation.

5. Acknowledgment

This work was supported by the National Natural Science Foundation of China (No.21371173，51402298) and China Postdoctoral Foundation (No. 2014M550846).

Notes and references

1. C. A. Grimes, O. K. Varghese, S. Ranjan, in *Light, Water, Hydrogen:The Solar Generation of Hydrogen by Water Photoelectrolysis; Springer Science+Business Media, LLC: New York,* **2008**.
2. A. Maria, L. Panagiotis, *J. Photochem. Photobio. A: Chem.* **2009***, 204,*69.
3. M. Antoniadou, V. M. Daskalaki, N. Balis, D. I. Kondarides, C. Kordulis, P. Lianos, *Appl. Catal. B* **2011**,*107*,188.
4. X. Meng, Y. Lu, B. Yang, G. Yi, J. Jia, *ACS Appl. Mater. Interfaces.* **2010**, *2*, 3467.
5. H. B.Yildiz, R. Tel-Vered, I. Willner, *Adv. Funct. Mater.* **2008**, *18*, 3497.
6. M. Shalom, I. Hod, Z. Tachan, S. Buhbut, S. Tirosh, A. Zaban, *Energy Environ. Sci.* **2011**, *4*, 1874.
7. J. C. Lee, W. Lee, S. H. Han, T. G. Kim, Y. M. Sung, *Electrochem. Commun.* **2009**, *11*, 231.
8. Y. K. Kim, H. Park, *Energy Environ. Sci.* **2011**, *4*, 685.
9. D. Kannaiyan,; E. Kim, N. Won, K. W Kim, Y. H. Jang, M.A. Cha, D. Y. Ryu, S. Kim, D. A. Kim, *J. Mater. Chem.* **2010**, *20*, 677.
10. D. Xi, H. Zhang, S. Furst, B. Chen, Q. Pei, *J. Phys. Chem. C* **2008**, *112*, 19765.
11. F. X. Xiao, J. W. Miao, B. Liu, J. Am. Chem. Soc., 2014, 136, 1559
12. J. T. Rhule, C. L Hill, D. A. Judd, *Chem. Rev.* **1998**, *98*, 327.
13. Z. X. Sun, F. Y. Li, L. Xu, S. P. Liu, M. L. Zhao, B. B. Xu, *J. Phys. Chem. C* **2012**, *116*, 6420.

14. Q. Xiang, J. Yu, M. Jaroniec, *Chem. Soc. Rev.* **2012**, *41*, 782.

15. X. Huang, X. Qi, F. Boey, H Zhang, *Chem. Soc. Rev.* **2012**, *41*, 666.

16. I. V. Lightcap, T. H. Kosel, P. V. Kamat, *Nano Lett.* **2010**, *10*, 577.

17. W. Han, L. Ren, L. Gong, X. Qi, Y. Liu, L. Yang, X. Wei, J. Zhong, *ACS Sustainable Chem. Eng*. 2014, 2, 741

18. L. Ren, X. Qi, Y. Liu, Z. Huang, X. Wei, J. Li, L. Yang, J. Zhong, *J. Mater. Chem.* 2012, 22, 11765

19. H. Li, S. Pang, S. Wu, X. Feng, K. Mullen, C. Bubeck, *J. Am.Chem. Soc.* **2011**, *133*, 9423.

20. D. Li, M. B. Muller, S. Gilje, R. B. Kaner, G. G. Wallace, *Nat.Nanotechnol.* **2008**, *3*, 101.

21. H. N. Kim, T. W. Kim, K. H. Choi, I. Y. Kim, Y. R. Kim, S. J. Hwang, *Chem.–Eur. J.* **2011**, *17*, 9626.

22. M. Sadakane, E. Steckhan, *Chem. Rev.* **1998**, *98*, 219.

23. R. N. Biboum, F. Doungmene, B. Keita, P. Oliveira, L. Nadjo, B. Lepoittevin, P. Roger, F. Brisset, P. Mialane, A. Dolbecq, I. M. Mbomekalle, C. Pichon, P. Yin, T. Liu, R. Contant, *J. Mater. Chem.* **2012**, *22*, 319.

24. H. Li, Y. Yang, Y. Wang, W. Li, L. Bi, L. Wu, *Chem. Commun.* **2010**, *46*, 3750.

25. Q. Li, B. D. Guo, J. G. Yu, J. R. Ran, B. H. Zhang, H. J. Yan, J. R. Gong, *J. Am. Chem. Soc.* **2011**, *133*, 10878.

26. M. Antoniadou, P. Lianos, J. Photochem. Photobio. A: Chem., 2009, 204,69

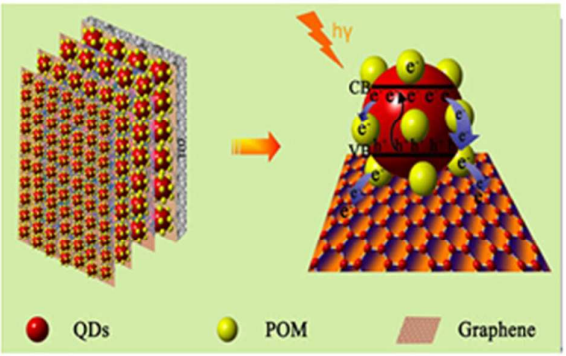

The rGO/CdS/H2W12 nanocomposite film was successfully fabricated by the layer-by-layer self-assembly method. The film showed strong ability of degradation of pollutant substance and production of hydrogen in the same time at low bias voltage under irradiation of solar light.